Jordan Journal of Civil Engineering, Volume **14**, No. **2**, **2020**

Strength of Steel Fiber High-strength Reinforced Concrete Columns under Concentric and Eccentric Loads

Saad Ali Al-Taan [1)] ***and Abdul Jalil Sulaiman Ahmad AlDoski*** [2)]

[1)] Professor, Civil Engineering Department, Mosul University, Mosul, Iraq.
E-Mail: saad.altaan49@gmail.com
[2)] Ph.D. Student, Dept. of Civil Engineering, Mosul University, Mosul, Iraq.
E-Mail: bawer85@yahoo.com

ABSTRACT

This paper presents test results on 20 square high-strength steel fiber-reinforced concrete columns 125×125×710 mm subjected to concentric and eccentric compression loading. The experimental program was mainly designed to examine the effect of the weight of steel fibers on the behavior of reinforced HSC columns subjected to axial and eccentric compression loading. All columns were longitudinally reinforced with 4 steel bars of 10 mm diameter and steel ties at 64 mm spacing. The test variables studied herein are the steel fiber weight percentage (0, 1.2, 2.4 and 3.6) and the eccentricity (0, 16, 32, 48 and 64mm). The test results showed that adding short discrete fibers to HSC mixtures in reinforced concrete columns not only prevents premature spalling of the concrete cover, but also increases the strength of the axially and eccentrically loaded reinforced columns.

This behavior was predicted also by the proposed method that is based on strain compatibility, equations of equilibrium, concrete strength in compression, longitudinal reinforcement ratio, steel fiber content and friction bond strength of the fibers. The stress blocks in compression recommended by the ACI and the CAN are adopted in this method. Predictions were found to be in good agreement with the experimental results.

KEYWORDS: Axial compression, Concrete columns, Eccentric compression, High-strength concrete, Steel fibers.

INTRODUCTION

The use of high-strength concrete (HSC) has been increasing for the last decades due to the ongoing development of concrete technology and the advantages of HSC over normal-strength concrete (NSC). HSC is primarily used in high-rise buildings (ACI-441R-1996), where it significantly reduces the dimensions of lower-story columns and the concrete volume for the entire building. Studies have shown, however, that HSC is more brittle in compression than NSC. The rate of heat transfer increases with compressive strength (Atea, 2017) and the confinement provided by lateral reinforcement to HSC is less effective than in NSC (Cusson and Paultre, 1994; Razvi and Saatcioglu, 1994; Pessiki and Pieroni, 1997) and this behavior is limiting the spread of its use.

The inclusion of short discrete fibers into the concrete mixtures can increase compressive strength and ductility of concrete, as already demonstrated by several studies (Hsu and Hsu, 1994; Mansur et al., 1999; ACI -544, 2002; Sharma, 2017).

The test results of 3 square large-scale reinforced HSC columns tested by Cusson and Paultre (1994) were reported by Paultre et al. (2010) who tested other 12 columns of the same dimensions (235× 235×1400 mm) with crimped steel fibers (40×0.8 mm) under axial compression loading. Two columns were tested with 0.25%, four with 0.5%, two with 0.75% and four with 1% by volume of steel fibers. The results showed that adding steel fibers to HSC mixtures in reinforced concrete columns not only prevents premature spalling of concrete cover, but also increases strength and

Received on 2/2/2019.
Accepted for Publication on 21/3/2020.

ductility of axially loaded columns.

Foster and Attard (2001) tested 9 high-strength, fiber-reinforced square columns with a side length of 155 mm and 12 square columns with a side length of 200 mm. The concrete mixture contained 2% by weight of end-hooked steel fibers (36×0.4 mm) and the concrete strength ranged from 67 to 88 MPa. The columns were tested at eccentricities of 0, 5, 8, 10, 20, 30 and 50 mm. The test results showed that the inclusion of steel fibers into concrete arrested early spalling of the cover and increased load capacity as well as ductility of the tested columns over those of comparable columns without steel fibers.

Tokgoz and Dundar (2011) tested 16 HSC reinforced composite columns with steel fiber volume percentage of (0, 0.5, 0.75 and 1.0) subjected to eccentric loads. A method for the analysis of these columns was proposed. The method was based on equilibrium, compatibility of strains, reinforcement properties, plain and fiber concrete in compression. The main parameters of this study were concrete compressive strength, load eccentricity, steel yield stress, slenderness effect and steel fiber content. The predicted to the test ultimate strength of these columns ranged from 0.851 to 1.052. The results showed that adding steel fibers into high-strength concrete significantly improves ductility and deformability of reinforced concrete and composite columns under biaxial bending and axial load.

Perceka et al. (2016) tested 9 small-scale 200× 200×900mm and 8 large-scale 400× 400× 1200 mm steel fiber HSC columns subjected to concentric compression load. Three different fiber volume fractions (0.75%, 1% and 1.5%) of (0.38×30 mm) and a volumetric transverse reinforcement ratio between 0 and 7.92% were used. Toughness ratio (TR) to quantify the confinement efficiency of HSC columns with hybrid confinement was proposed through a regression analysis by involving sixty-nine TRs of HSC without steel fibers and twenty-seven TRs of HSC with a hybrid of transverse reinforcement and steel fibers. The results showed that the efficiency of steel fibers in concrete depends on transverse reinforcement spacing, where steel fibers are more effective if the spacing of transverse reinforcement becomes larger in the range of (0.25–1) effective depth of the column section.

Hadi et al. (2017) reported the test results of 16 circular HSC columns of 205 mm diameter and 800 mm height reinforced with either micro-, macro- or hybrid steel fibers. All the specimens were longitudinally reinforced with six 12-mm diameter bars and 6-mm diameter helix. The specimens contained a volume percentage of steel fibers of either 0%, 3% micro-fibers (0.2×6 mm), 2.5% macro-fibers (0.55×18 mm) or hybrid (1.5% micro- + 1% macro-) fibers. The specimens were tested under concentric, 25 and 50 mm eccentric and four-point bending. The test results showed that inclusion of either micro- or hybrid steel fibers into HSC enhanced strength and ductility of the tested columns under eccentric axial loads. The results also showed that the addition of macro-steel fibers into HSC enhanced ductility, but reduced strength of specimens compared to specimens without steel fibers.

The aim of this study is to determine the influence of steel fiber content on the strength and behavior of HSC specimens under concentric and eccentric loads and propose a method for predicting the strength of such columns.

Research Significance

The objective of this study is to investigate the effect of steel fiber content on the behavior and strength of HSC column specimens under concentric and eccentric loads. Also, the effects of steel fibers in tension were taken into account in the proposed method to determine axial load and bending moment capacity of HSC columns.

EXPERIMENTAL PROGRAM

Test Specimens and Designation

The experimental program was designed to investigate the effect of steel fibers on the behavior of HSC column specimens under concentric load and (16 mm, 32 mm, 48 mm and 64 mm) eccentric compression loads. Twenty specimens were cast and tested. In this study, the same specimen sizes were tested under different loading conditions to avoid the size effect on the experimental results. Square specimens with (125 mm) side length and (710 mm) height were designed to avoid the formation of secondary moments due to slenderness effect. The two specimen ends were enlarged to a size of (125×175mm) and reinforced as shown in Fig. (1) to

avoid premature failure. The dimensions were chosen to be suitable to the condition and capacity of the available testing facility in the laboratory. The concrete cover on each side of the ties as well as at the top and bottom of the specimens was (15 mm).

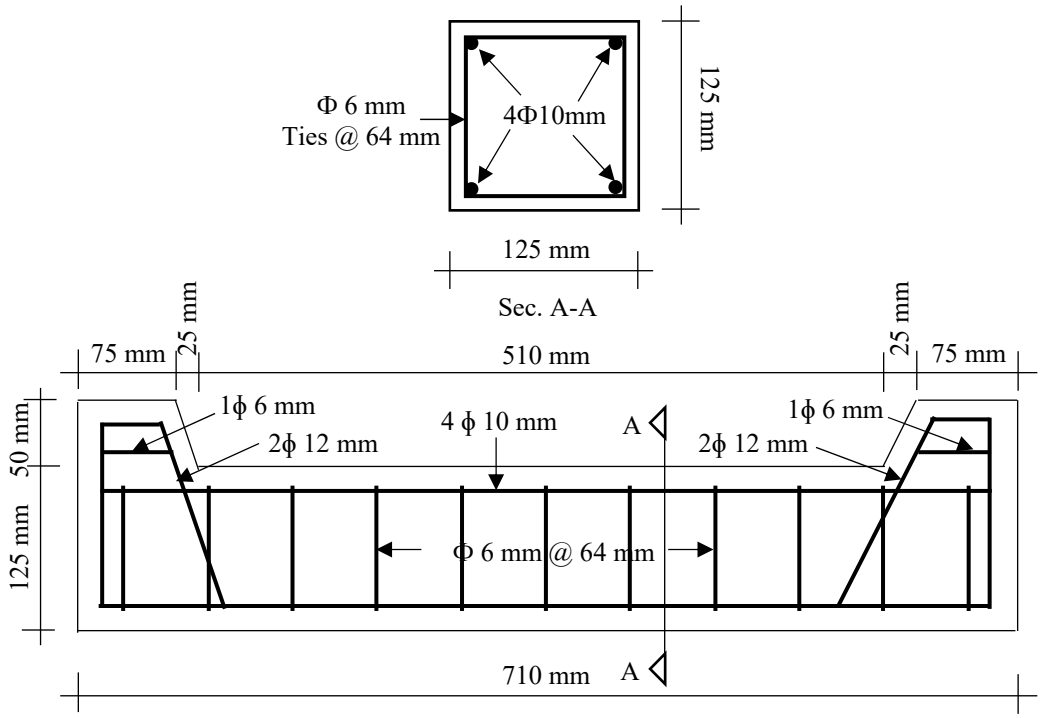

Figure (1): Details of the reinforced concrete columns

The specimens were divided into five groups each containing four columns. The first group was tested under concentric compression, the second under (16mm) eccentric load, the third under (32 mm) eccentric load, the fourth under (48 mm) eccentric load and the fifth under (64 mm) eccentric load. The first specimen in each group contained no steel fibers, the second contained 1.2%, the third contained 2.4% and the fourth contained 3.6% by weight of steel fibers.

Specimens were designated by one letter and two numbers, where the first letter refers to the specimen, the second to the eccentricity and the third to the steel fiber weight percentage. The specimens were tested until failure using 3000 kN compression machine. All specimens were cast and tested at the age of (56 days) in the Structural Engineering Laboratory of the Department of Civil Engineering, University of Duhok, Iraq.

MATERIAL PROPERTIES

The target compression strength was 90 MPa. Many trial mixes were conducted to obtain HSC (ACI 363-2010). The final mix proportions are shown in Table (1). Type 1 ordinary Portland cement conforming to (ASTM C150-2011), crushed gravel of (10 mm) maximum size conforming to (ASTM C33-2003), river sand conforming to (ASTM C33-2003) and silica fume meeting the requirements of (ASTM C1240-2003) were used to produce HSC. To improve the workability of the concrete mixtures, an adequate amount of hyperplast PC200 which is a high-range water-reducing admixture was added in compliance with (ASTM C494-2004).

Table 1. Mixture proportions by weight

Cement	Sand	Gravel	W/C	Silica fume	Superplasticizer
1	1.15	1.50	0.30	0.15	0.015

Plate (1): Copper-coated steel fibers

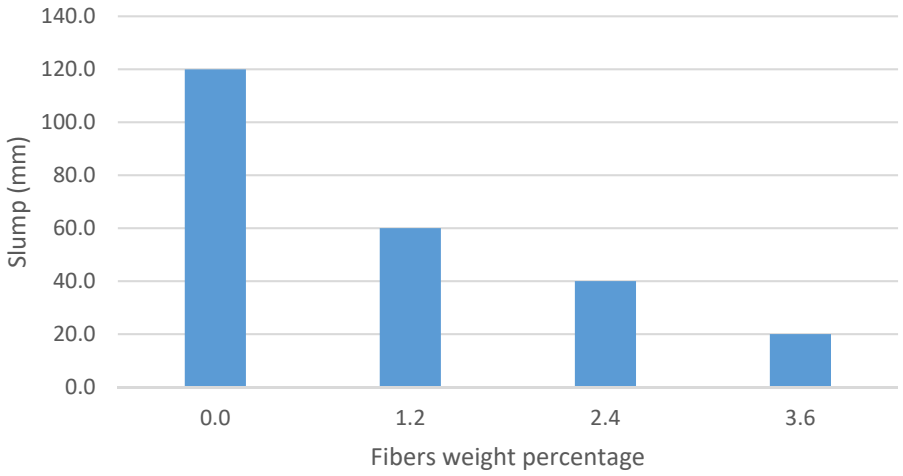

Figure (2): Variation of slump with fiber weight percentage

Plate (2): Steel molds and reinforcement cag

Copper-coated steel fibers were used to reinforce the specimens, which are (13 mm) long and (0.2 mm) in diameter with a nominal tensile strength of (2850 MPa) as provided by the manufacturer and complying with (ASTM A820-2011), Plate (1). The specimens were longitudinally reinforced with four deformed steel bars of (10 mm) diameter (ρ_g = 0.0195) having a yield strength of (573 MPa). For ties, deformed steel bars of (6 mm) diameter with yield strength = (598 MPa) spaced at (64 mm = 0.65×effective depth) were used to make the steel fibers effective as proposed by Perceka et al. (2016). Fig. (1) shows the dimensions and the reinforcement arrangement of the specimens. Six cylinders with (100 mm) diameter and (200 mm) height and three prisms (100×100×400 mm) were cast and tested to determine compressive, splitting and flexural strength, respectively, for the four concrete mixtures.

The workability of the HSC mixtures was determined using the slump test. The results of the slump test of the four fresh mixes are presented in Fig. (2). It can be seen from Fig. (2) that the slump values of HSC mixes reinforced with steel fibers reduced with the increase in weight content of steel fibers.

Preparation and Casting Procedure

Column specimen formworks were made from steel, Plate (2). The deformed (10 mm) steel bars were cut to a length to have (15 mm) clear cover at the top and the bottom of the reinforcement cage. Square ties with an outside length of (95 mm) and (64 mm) were used as lateral reinforcement.

The concrete mixture was placed in the formwork in two layers, six cylinders and three prisms and vibrated by table vibration to remove air pockets. Finally, the surface was finished with a wet trowel.

After casting, all specimens were covered with nylon sheet to prevent moisture loss. The specimens were removed from the molds (24 hours) after casting and immersed in a water curing tank for (52 days). The specimens were then taken out of water and left in the laboratory for two days, cleaned and painted with white emulsion to observe cracks and crack propagation. The day after, strain gauges were fixed on the concrete surface on two opposite edges (mid-height) to measure the compression strains for axially loaded specimens and compression and tension strains for eccentrically loaded specimens. The top and bottom ends of all column specimens were leveled by using sulfur capping. The columns were tested at the age of 56 days.

Instrumentation and Testing Procedure

A circular bar of 20 mm diameter between two steel plates with dimensions of (235×185 mm) and thickness of (20 mm) was placed at the top and bottom of column specimens in order to distribute the compression loads. Circular grooves 4 mm deep (radius = 20 mm) were provided in the outer plates and five grooves were spaced 16 mm on centers in the inner plates (in contact with the column) to provide the required eccentricity, Fig. (3).

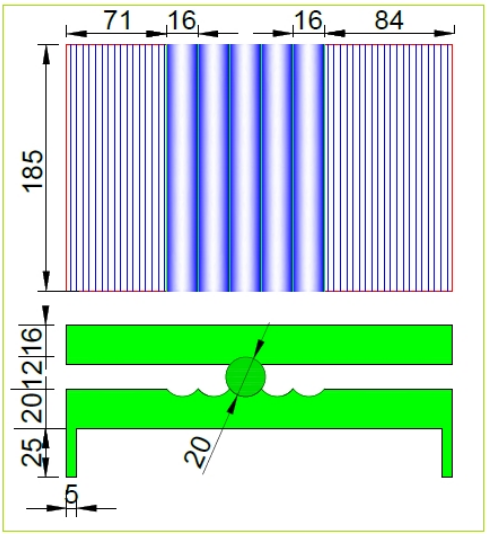

Figure (3): Steel plates above and below the columns

Plate (3): Apparatus used for the test

The specimens were internally instrumented before casting of concrete to measure axial strains. Two electrical strain gauges were attached at mid-height of the longitudinal bars on the two opposite sides to capture axial strains in the longitudinal bars.

For eccentrically loaded specimens, LVDT was placed at the column mid-height to measure the lateral deflection of the specimens. All specimens were tested under a constant loading rate of 0.3 kN/sec.

RESULTS AND DISCUSSION

Table (2) shows the details of concrete strength, failure loads and percentage increase in the column strength due to steel fiber addition. Compression strength splitting strength and flexural strength of concrete increased due to fiber addition up to 12%, 52% and 43%, respectively. The difference in the enhancement of the three strengths is attributed to the different failure mechanisms (Thomas and Ramaswamy, 2007). The increase in column strength due to fiber addition ranged from 1.31% to 11.58%.

For the axially loaded columns (S00, S01.2, S02.4 and S03.6), the load carried by the steel bars is calculated from the measured steel strains, Fig. (4). The figure shows a marginal decrease of the load with the steel fiber percentage, which may be attributed to the minor increase in compression strength of concrete. The average percentage of load carried by the steel bars was equal to 9.1%. This figure is in agreement with the value of 10% which was found by Afifi (2013) for circular columns reinforced with 1.7% steel bars.

For the axially loaded columns (S00, S01.2, S02.4 and S03.6), the increase in load-carrying capacity of the columns due to steel fiber addition is not proportional to the compression strength of concrete, but approximately to the increase of the load carried by concrete, if the load carried by the steel reinforcement is excluded as shown in Table (3).

For the eccentrically loaded columns (S160, S161.2, S162.4 and S163.6), the whole cross-section is in compression and the computed neutral axis depth is more than the column depth, as shown in Table (5). The increase in the column strength due to steel fiber addition ranged between 1.3% and 10.5%, which is slightly less than that for the axially loaded columns.

For other values of eccentricities (32, 48 and 64 mm), where there are compression and tension zones and the stress resultant will be increased marginally in compression and in tension, there will be an increase due to the tension stiffening of the steel fibers and the net increase in the column carrying capacity is the algebraic sum of the negative stress (compression) and the positive stress (tension) resultant. The increase in the column strength does not show any trend with eccentricity.

Table 2. Mechanical properties of the concrete mixtures and failure loads of the columns

Spec. ID	e (mm)*	W_f %**	Strength (MPa)			Failure load kN	Inc. in str. due to fiber addition %
			$f_c'^{+}$	f_{sp}^{++}	$f_r^{\#}$		
S00	0	0	94.3	6.92	10.13	1551.0	
S01.2	0	1.2	99.6	9.10	13.77	1598.0	3.03
S02.4	0	2.4	102.9	9.12	14.02	1648.0	6.25
S03.6	0	3.6	105.6	10.49	14.51	1664.0	7.29
S160	16	0	94.3	6.92	10.13	1141.0	---
S161.2	16	1.2	99.6	9.10	13.77	1156.0	1.31
S162.4	16	2.4	102.9	9.12	14.02	1257.0	10.17
S163.6	16	3.6	105.6	10.49	14.51	1261.0	10.52
S320	32	0	94.3	6.92	10.13	757.0	---
S321.2	32	1.2	99.6	9.10	13.77	781.0	3.17
S322.4	32	2.4	102.9	9.12	14.02	796.0	5.15
S323.6	32	3.6	105.6	10.49	14.51	799.0	5.55
S480	48	0	94.3	6.92	10.13	475.0	---
S481.2	48	1.2	99.6	9.10	13.77	509.0	7.16
S482.4	48	2.4	102.9	9.12	14.02	516.0	8.63
S483.6	48	3.6	105.6	10.49	14.51	530.0	11.58
S640	64	0	94.3	6.92	10.13	359.0	---
S641.2	64	1.2	99.6	9.10	13.77	362.0	0.84
S642.4	64	2.4	102.9	9.12	14.02	369.0	2.79
S643.6	64	3.6	105.6	10.49	14.51	375.0	4.46

- Eccentricity, **fiber weight, +cylinder compression strength, ++ splitting strength, # flexural strength.

Table 3. Comparison between compression strength of concrete and experimental failure loads for axially loaded columns

Specimen ID	S00	S01.2	S02.4	S03.6
f_c' (MPa)	94.3	99.6	102.9	105.6
% increase in f_c'	---	5.6	9.1	12
Exp. failure load kN	1551.0	1598.0	1648.0	1664.0
% increase in the exp. load due to steel fibers	---	3.03	6.25	7.29
Load carried by the steel bars	156.53	153.85	144.47	134.45
Load carried by the concrete	1394.47	1444.15	1503.53	1529.55
% increase in the load carried by concrete	---	3.56	7.82	9.69

Table 4. Summary of experimental and predicted ultimate loads

Spec. ID	Exp. load	Predicted N.A. Depth and Ultimate Loads				Exp. / Calc. Can. code	Exp. / Calc. ACI code
		CAN. Code		ACI Code			
	kN	c (mm)	kN	c (mm)	kN		
	1	2	3	4	5	1/3	1/5
S00	1551	∞	1198.2	∞	1402.5	1.294	1.106
S01.2	1598	∞	1243.6	∞	1471.6	1.285	1.086
S02.4	1648	∞	1271.2	∞	1514.5	1.296	1.088
S03.6	1664	∞	1293.4	∞	1549.7	1.287	1.074

S160	1141	127.6	881.1	142.5	1018.4	1.295	1.120
S161.2	1156	129.7	915.5	142.4	1069.2	1.264	1.081
S162.4	1257	131	936.1	142.4	1101.2	1.343	1.141
S163.6	1261	132.1	952.6	142.4	1127.4	1.324	1.119
S320	757	88.7	596.8	96	676.8	1.268	1.118
S321.2	781	89.9	617.7	96.1	710.4	1.264	1.099
S322.4	796	90.8	630.7	96.2	731.0	1.262	1.089
S323.6	799	91.6	640.7	96.4	748.2	1.247	1.068
S480	475	65.8	404.0	67.0	436.7	1.176	1.088
S481.2	509	66.5	416.6	67	456.9	1.222	1.140
S482.4	516	67	424.0	67.2	469.9	1.217	1.098
S483.6	530	65.4	430.0	67.4	480.8	1.233	1.102
S640	359	55	298.0	53.9	310.5	1.205	1.156
S641.2	362	55.3	305.6	53.8	323.8	1.185	1.118
S642.4	369	55.7	310.3	53.9	332.5	1.189	1.109
S643.6	375	56.1	314.4	54.1	339.7	1.193	1.104
Average $P_{exp.}$ / $P_{cal.}$						1.257	1.104
Standard deviation						0.049	0.022
Coefficient of variation %						3.92	1.97

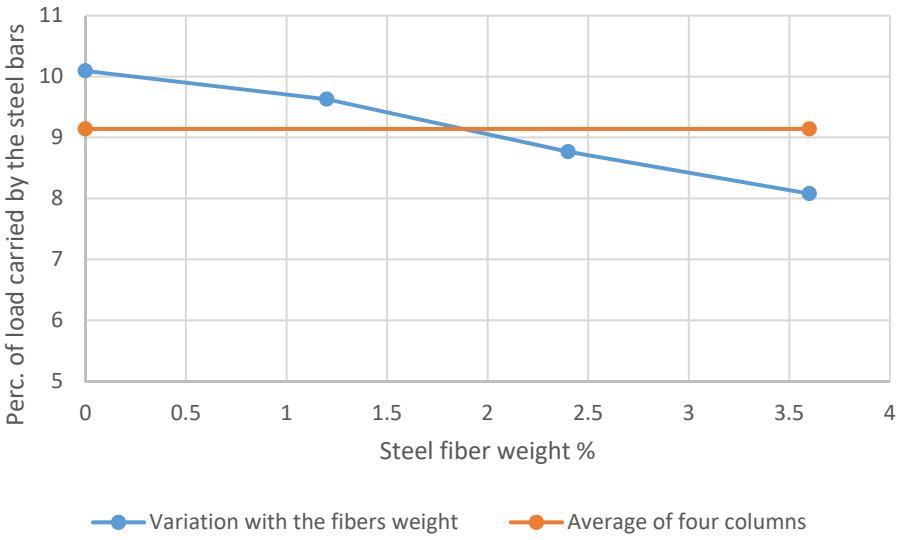

Figure (4): Variation of load carried by steel bars with steel fiber weight for axially loaded columns (Series S)

Column Failure Mode

In the four axially loaded columns (S00, S01.2, S02.4 and S03.6) and the four columns with e = 16 mm (S160, S161.2, S162.4 and S163.6), the whole cross-section is subjected to compression stresses and the columns failed in compression as shown in Fig. (5a, b). Columns with eccentricities of 32 mm and 48 mm are in the compression-controlled region of the failure envelope and failed in a bending mode, where the ultimate concrete compression strains reached their maximum before the tension steel reached its yield strains, as shown in Tables (6, 7). Columns with e = 64 mm are in the tension- controlled region of the failure envelope and failed also in a bending mode, but with the tensile steel yield strains attained before the columns reached their failure state, as shown in Tables (6, 7). Fig. (5a, b, c, d and e) shows that columns without steel fibers exhibited spalling of the concrete

cover at failure, while those with steel fibers did not exhibit any spalling and retained the integrity of the columns as shown in Fig. (5f, g, h, i, j).

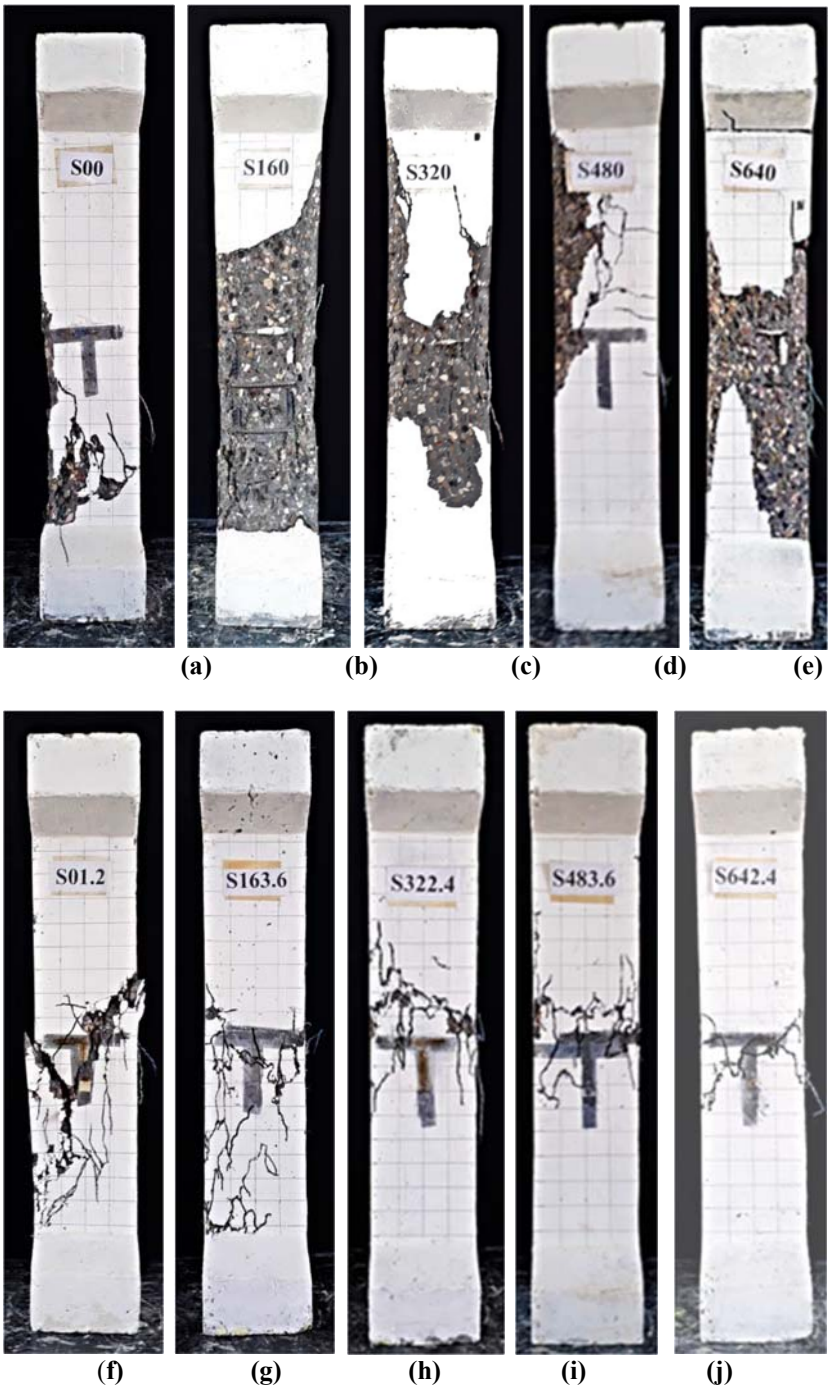

Figure (5): Failed columns, (a) S00, (b) S160, (c) S320, (d) S480, (e) S640, (f) S01.2, (g) S163.6, (h) S322.4, (i) S483.6 and (j) S642.4

Steel and Concrete Strains

Tables (6, 7) show the measured and predicted steel and concrete strains. The predicted strains are calculated on the assumption of linear strain distribution and the ultimate concrete strain in compression = (0.003) and (0.0035) as recommended by (ACI 318-14) and (CAN. Standards, 2004). Tables (6, 7) exhibit that the steel and concrete compression

strains show better agreement than those in tension and this may be attributed to the continuity and homogeneity of compression zones, while tension zones contain cracks that disrupt the continuity and linearity of strains.

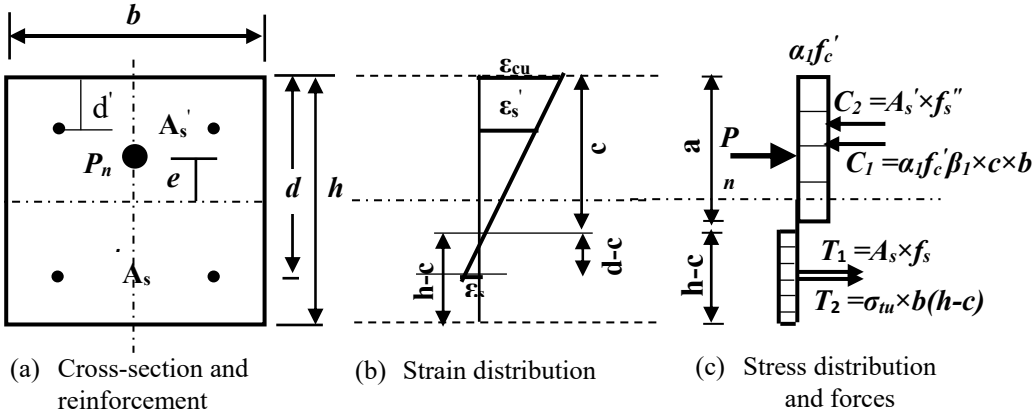

Figure (6): (a) Cross-section and reinforcement, (b) Strain distribution and (c) Stress distribution and forces

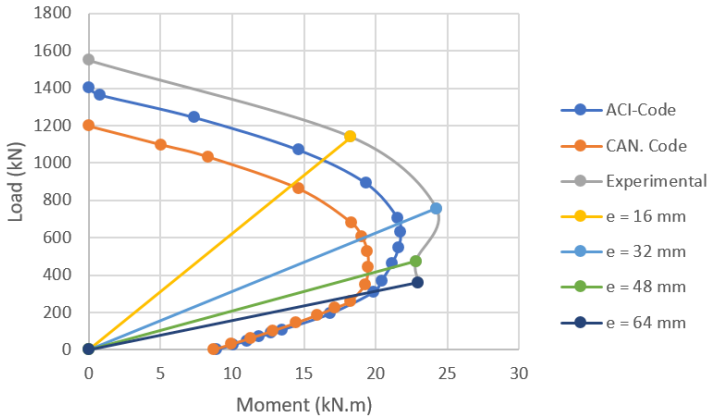

Figure (7): Experimental and predicted interaction diagrams ($W_f = 0$)

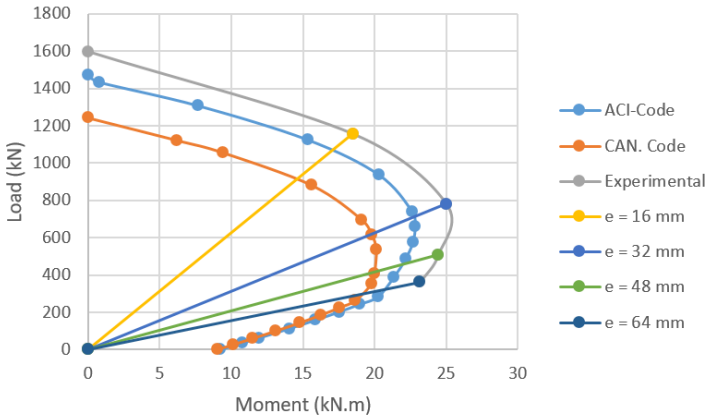

Figure (8): Experimental and predicted interaction diagrams ($W_f = 1.2\%$)

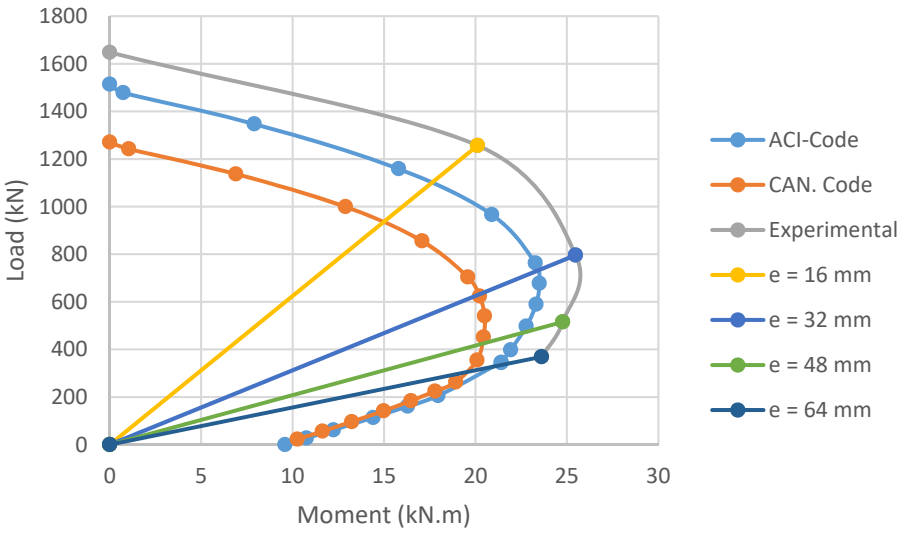

Figure (9): Experimental and predicted interaction diagrams (W_f = 2.4%)

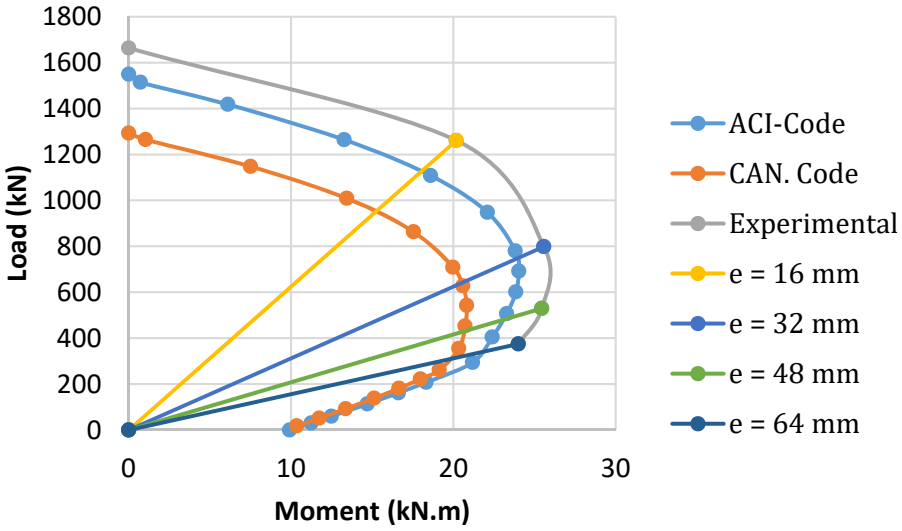

Figure (10): Experimental and predicted interaction diagrams (W_f = 3.6%)

Predicted Values of Column Strength

The procedure used for the analysis of the tested columns is that used for conventionally reinforced concrete columns using the strength design method recommended by (ACI Code 318-14) and (CAN. Standards, 2004) and the contribution of the steel fibers in the tension zone, Fig. (6). Post-cracking tensile strength of steel fiber concrete (σ_{tu}) is estimated as:

$$\sigma_{tu} = \eta_o \times \tau_u \times V_f \times L_f / D_f \qquad (1)$$

where η_o = orientation factor representing the percentage of fibers oriented in a certain direction. Values of 0.333, 0.41 and 0.5 were proposed for this factor and the value of 0.5 is used in this investigation (Hannant, 1978), τ_u = interfacial bond strength between steel fibers and concrete and the relationship proposed by Ng et al. (2012) is used in this investigation:

$$\tau_u = k_s \sqrt{f_c'} \qquad (2)$$

where k_s = shape factor equal to 0.4 for smooth plain fibers and 0.8 for shaped fibers, such as end-hooked, crimped or deformed fibers, V_f, L_f and D_f are the volume fraction, length and diameter of the fibers, respectively. The maximum compression strain (ε_{cu}) is equal to 0.003 as recommended by (ACI 318-14, 2014) and 0.0035 as recommended by (CAN. Standards, 2004). α_1 and β_1 are as shown below:

$$\alpha_1 = 0.85 \quad \text{(ACI 318-14)} \tag{3a}$$

$$\alpha_1 = 0.85 - 0.0015 f_c' \geq 0.67 \quad \text{(CAN. Standards, 2004)} \tag{3b}$$

$$\beta_1 = 0.85 - 0.00725(f_c' - 28) \geq 0.65 \quad \text{(ACI 318-14)} \tag{4a}$$

$$\beta_1 = 0.85 - 0.0025 f_c' \geq 0.67 \quad \text{(CAN. Standards, 2004)} \tag{4b}$$

The calculated ultimate loads and the neutral axes depths together with measured ultimate loads results are shown in Table (5). The predicted values of the ultimate loads using [ACI Code (318-14)] are higher than the values predicted using [CAN. Standards, 2004] by about 4% to 20% and this may be attributed to the following reasons:

i. The value (α_1 = 0.85) in Equation (3a) recommended by (ACI 318-14) is higher than the value of (α_1, ranging from 0.69 to 0.71) in Equation (3b) recommended by (CAN. Standards, 2004),
ii. The value (β_1 = 0.65) for HSC in Equation (4a) recommended by (ACI 318-14) is lower than the value of (β_1, ranging from 0.71 to 0.73) in Equation (4b) recommended by (CAN. Standards, 2004) and
iii. The product ($\alpha_1 \times \beta_1$) using (ACI 318-14) is about 10% higher than the product ($\alpha_1 \times \beta_1$) using the (CAN. Standards, 2004).

Table 5. Difference between average values of experimental to predicted failure load between the (ACI 318-14) and (CAN. Standards, 2004)

Eccentricity (mm)	0	16	32	48	64
Difference %	20.3	19.1	16.6	13.2	7.1

Table 6. Calculated and measured ultimate steel strains

Specimen ID	**Tension steel**			**Compression steel**		
	Calculated strains (μs)		**Measured strains (μs)**	**Calculated strains (μs)**		**Measured strains (μs)**
	ACI	**CAN.**		**ACI**	**CAN.**	
S00	-3000	-3500	-2219	-3000	-3500	-2920
S01.2	-3000	-3500	-2141	-3000	-3500	-2910
S02.4	-3000	-3500	-1909	-3000	-3500	-2834
S03.6	-3000	-3500	-1639	-3000	-3500	-2775
S160	-672	-1068	-822	-2453	-2787	-2822
S161.2	-710	-1067	-723	-2452	-2798	-2786
S162.4	-733	-1067	-612	-2452	-2805	-2631
S163.6	-753	-1067	-643	-2452	-2811	-2524
S320	348	109	1100	-2188	-2474	-2632
S321.2	304	106	900	-2188	-2488	-2585
S322.4	271	102	810	-2189	-2498	-2457
S323.6	242	94	610	-2191	-2507	-2351
S480	1514	1672	2908	-1836	-2117	-2351
S481.2	1466	1672	2662	-1836	-2132	-2189
S482.4	1433	1656	2559	-1839	-2142	-2116
S483.6	1541	1641	2183	-1843	-2109	-1967
S640	2400	2929	4335	-1553	-1845	-2219
S641.2	2371	2941	4102	-1550	-1854	-1993
S642.4	2332	2929	3598	-1553	-1866	-1794
S643.6	2294	2905	3197	-1558	-1878	-1763

Table 7. Calculated and measured ultimate concrete strains

Specimen ID	Tension face			Compression face		
	Calculated strains (μs)		Measured strains (μs)	Calculated strains (μs)		Measured strains (μs)
	ACI	CAN.		ACI	CAN.	
S00	-3000	-3500	-2447	-3000	-3500	-3568
S01.2	-3000	-3500	-2125	-3000	-3500	-3445
S02.4	-3000	-3500	-2104	-3000	-3500	-3307
S03.6	-3000	-3500	-1859	-3000	-3500	-3154
S160	-71	-368	-271	-3000	-3500	-4007
S161.2	-127	-367	-247	-3000	-3500	-3983
S162.4	-160	-367	-219	-3000	-3500	-3845
S163.6	-188	-367	-106	-3000	-3500	-3533
S320	1432	906	4897	-3000	-3500	-4126
S321.2	1367	902	3570	-3000	-3500	-4063
S322.4	1318	898	3367	-3000	-3500	-3912
S323.6	1276	890	3087	-3000	-3500	-3634
S480	3149	2597	6639	-3000	-3500	-4358
S481.2	3079	2597	6179	-3000	-3500	-4198
S482.4	3030	2580	5736	-3000	-3500	-4005
S483.6	3190	2564	5135	-3000	-3500	-3862
S640	4455	3957	4121	-3000	-3500	-4559
S641.2	4411	3970	4647	-3000	-3500	-4325
S642.4	4355	3957	5438	-3000	-3500	-4104
S643.6	4299	3932	6148	-3000	-3500	-3896

However, this is more pronounced in the axially loaded columns or columns with small eccentricity.

In the present study, however, recommendations gave safe and conservative prediction of the ultimate load for all values of eccentricities. The calculated values of the neutral axes depth using (ACI 318-14) are higher than those using (CAN. Standards, 2004) for the first three values of eccentricities (e = 0, 16 and 32 mm), where the compression zone extends over more than 70% of the cross-section. This can be attributed to the same two reasons mentioned above. For higher values of eccentricity (e = 48 and 64 mm), the area under compression is decreased and the effect of the parameters (α_1 and β_1) in Equations (3, 4) is minimized.

Table (7) shows the average difference between the predicted values of the failure loads. It can be noticed that the difference decreased with the increased eccentricity, where the area under compression is minimized and the influence of the parameters (α_1 and β_1) in Equations (3, 4) is decreased also as mentioned above.

Predicted and Experimental Interaction Diagrams

The analysis procedure adopted is used to plot the interaction diagrams, using both (CAN. Standards, 2004), (ACI 318-14) and the experimental results. Figs. (5-8) show the interaction diagrams for the four steel fiber weights (0, 1.2, 2.4 and 3.6%). As previously mentioned, (ACI 318-14) gave higher values of column load-carrying capacity than (CAN. Standards, 2004), especially for lower values of eccentricity due to the reasons previously stated. The figures show also that in the tension-controlled region (where the tension zone extends over more than 50% of the whole cross-section), there is no appreciable difference between the two diagrams due to the diminishing effect of the stress block parameters (α_1 and β_1).

For all the eccentricities, the calculated neutral axes depth values in Table (4) are higher than the balanced values and the experimental failure loads are more than the balanced values shown in Table (4) using [ACI 318-14], indicating a compression failure.

However, using (CAN. Standards, 2004), the balanced values of the neutral axis depth and the

balanced values of the loads are slightly higher than those using (ACI 318-14) and the neutral axis depth for (e = 64 mm) is approximately equal to the balanced value. This is more clearly indicated in the values of the steel strains in the tension steel shown in Table (6) which are more than the yield strain of 2865μs, indicating the end of the compression failure zone and the beginning of the tension zone.

CONCLUSIONS

Twenty square HSC specimens of 125 mm and 710 mm height with and without steel fibers were tested to investigate the influence of weight content of steel fibers on the strength. The specimens were tested under concentric and different eccentric loads. The main variables in the experimental program are the steel fiber content and the eccentricity of the applied axial load. Based on the experimental and theoretical results, the following conclusions can be drawn:

1. The inclusion of steel fibers into HSC column specimens increased the maximum axial load of concentrically and eccentrically loaded specimens.
2. The test results showed that premature concrete cover spalling of high-strength concrete columns can be delayed or prevented by using steel fibers.
3. Concrete and steel strains and deflections decreased with steel fiber content.
4. Concrete and steel strains and deflections were reasonably predicted by the proposed method.
5. The strengths of both concentrically and eccentrically loaded columns were satisfactorily predicted by the proposed method using (ACI 318-14) and (CAN. Standards, 2004).
6. The predicted strengths using (ACI 318-14) recommendations are higher than those using (CAN. Standards, 2004) and the difference diminishes with eccentricity.

REFERENCES

ACI Committee 441R. (1996). "State-of-the-art of high-strength concrete columns". American Concrete Institute, Farmington Hills, MI, 48331, USA.

ACI Committee 318. (2014). “Building code requirements for structural concrete (ACI 318-14) and commentary.” American Concrete Institute, Farmington Hills, MI, 48331, USA, 153-162 and 347-384.

ACI Committee 363R. (2010). “Report on high-strength concrete (ACI 363-10)”. American Concrete Institute, Farmington Hills, MI, 48331, USA.

ACI Committee 544. (2002). "State-of-the-art report on fiber-reinforced concrete ACI 544-02". American Concrete Institute, Farmington Hills, MI, 48331, USA.

Afifi, M.M.Z.M. (2013). "Behavior of circular concrete columns reinforced with FRP bars and stirrups". Ph.D. Dissertation, Sherbrooke University, Canada.

ASTM C33-03. (2003). “Standard specification for concrete aggregates”. (ASTM C33-03), American Society for Testing and Materials.

ASTM C150-11. (2011). “Standard specification for Portland cement”. (ASTM C150-11), American Society for Testing and Materials.

ASTM C494-4. (2004). “Standard specification for chemical admixtures for concrete”. (ASTM C 494-04), American Society for Testing and Materials.

ASTM A820-11. (2011). “Standard specification for steel fibers for fiber-reinforced concrete”. (ASTM A820-11), American Society for Testing and Materials.

ASTM C1240-03, (2003). “Standard specification for silica fume used in cementitious mixtures”. (ASTM 1240-03), American Society for Testing and Materials.

Atea, R. (2017). “Fire resistance performance of recycled aggregate concrete columns with direct concrete compressive strength”. Jordan Journal of Civil Engineering, 11 (3), 424-438.

Canadian Standard Association-CSA. (2004). “Design of concrete structures”. CSA A23.3-04, Canadian Standard Association, Mississauga, Ont.

Cusson, D., and Paultre, P. (1994). “High-strength concrete columns confined by rectangular ties”. J. Structural Engrg., ASCE, 120 (3), 783-804.

Foster, S. J., and Attard, M. M. (2001). “Strength and ductility of fiber-reinforced high-strength concrete columns". J. of Structural Engrg., 127 (1), 28-34.

Hadi, M.N.S., Balanji, E.K.Z., and Sheikh, M.N. (2017). "Behavior of steel fiber-reinforced high-strength concrete concrete columns under different loads". ACI Structural J., 114 (4), 1-12.

Hannant, D.J. (1978). Fibre cements and fibre concretes". John Wiley and Sons, Inc., New York.

Hsu, L.S., and Hsu, C.T.T. (1994). "Stress-strain behavior of steel-fiber high-strength concrete under compression." ACI Struct. J., 91 (4), 448-457.

Mansur, M. A., Chin, M. S., and Wee, T. H. (1999). "Stress-strain relationship of high-strength fiber concrete in compression". J. Mater. Civ. Engrg., 11 (1), 21-29.

Ng, T.S., Htut, T.N.S., and Foster, S.J. (2012). "Fracture of steel fiber-reinforced concrete: the unified variable engagement model". Report No. UNICIV R-460, School of Civil and Environmental Engrg., University of New South Wales, Sydney, Australia, 107 pp.

Paultre, P., Eid, R., Langlois, Y., and Lévesque, Y. (2010). "Behavior of steel fiber-reinforced high-strength concrete columns under uniaxial compression". J. of Structural Engrg., 136 (10), 1225-1235.

Perceka, W., Liao, W.C., and Yo-de Wang, Y.D. (2016). "High-strength concrete columns under axial compression load: hybrid confinement efficiency of high-strength transverse reinforcement and steel fibers". J. of Materials, 9 (264), 25 pp.

Pessiki, S., and Pieroni, A." Axial load behavior of large-scale spirally reinforced high-strength concrete columns". ACI Structural J., 94 (3), 304-314.

Razvi, S. R., and Saatcioglu, M. (1994). "Strength and deformability of confined high-strength concrete columns". ACI Structural J., 91 (6), 678-687.

Sharma, R. (2017). "Compression strength of concrete using construction demolition waste, glass waste, superplasticizer and fiber". Jordan Journal of Civil Engineering, 11 (3), 455-472.

Thomas, J., and Ramaswamy, A. (2007). "Mechanical properties of steel fiber-reinforced concrete". J. of Materials in Civil Engineering, 19 (5), 385-392.

Tokgoz, S., and Dundar, C. (2011). "Analysis of reinforced concrete and composite columns with and without steel fibers". Proceedings of the 2011 International Balkan Conference on Challenges of Civil Engineering, BCCCE, May 19th -21st, EPOKA University, Tirana, Albania. 9 pp.